

Characterization of the Mechanical and Thermal Properties and Morphological Behavior of Biodegradable Poly(L-lactide)/Poly(ϵ -caprolactone) and Poly(L-lactide)/Poly(butylene succinate-co-L-lactate) Polymeric Blends

V. Vilay,^{1,2} M. Mariatti,¹ Zulkifli Ahmad,¹ K. Pasomsouk,² Mitsugu Todo³

¹School of Materials and Mineral Resources Engineering, Engineering Campus, Universiti Sains Malaysia, 14300 Nibong Tebal, Seberang Perai Selatan, Pulau Pinang, Malaysia

²Department of Mechanical Engineering, National University of Laos, Vientiane, Lao People's Democratic Republic

³Research Institute for Applied Mechanics, Kyushu University, Fukuoka, Japan

Received 16 October 2008; accepted 17 April 2009

DOI 10.1002/app.30683

Published online 24 June 2009 in Wiley InterScience (www.interscience.wiley.com).

ABSTRACT: Two series of biodegradable polymer blends were prepared from combinations of poly(L-lactide) (PLLA) with poly(ϵ -caprolactone) (PCL) and poly(butylene succinate-co-L-lactate) (PBSL) in proportions of 100/0, 90/10, 80/20, and 70/30 (based on the weight percentage). Their mechanical properties were investigated and related to their morphologies. The thermal properties, Fourier transform infrared spectroscopy, and melt flow index analysis of the binary blends and virgin polymers were then evaluated. The addition of PCL and PBSL to PLLA reduced the tensile strength and Young's modulus, whereas the elongation at

break and melt flow index increased. The stress-strain curve showed that the blending of PLLA with ductile PCL and PBSL improved the toughness and increased the thermal stability of the blended polymers. A morphological analysis of the PLLA and the PLLA blends revealed that all the PLLA/PCL and PLLA/PBSL blends were immiscible with the PCL and PBSL phases finely dispersed in the PLLA-rich phase. © 2009 Wiley Periodicals, Inc. *J Appl Polym Sci* 114: 1784–1792, 2009

Key words: blends; mechanical properties; thermal properties

INTRODUCTION

Biodegradable polymers are receiving wide acceptance in various applications because of their unique and interesting properties, such as biocompatibility, mechanical properties, and biodegradability.^{1–4} A biodegradable polymer is defined as one that undergoes microbially induced chain scission leading to mineralization.⁵ The use of these materials in various applications may reduce the environmental problems caused by the wastes emanating from synthetic nondegradable polymers.⁶ As reported earlier, many studies have been carried out to examine the relationship between the structure and properties of various biodegradable polymers such as poly(L-lactide) (PLLA), poly(ϵ -caprolactone) (PCL), poly(butylene succinate), and poly(butylene succinate-co-L-lactate) (PBSL).^{1–7}

Among biodegradable polymers, much attention has been given to PLLA, a biodegradable polymer

derived from the starch of potato and corn. PLLA has strength and modulus comparable to those of commercially available engineering polymers. However, PLLA exhibits brittle fracture behavior, especially under impact loading conditions; therefore, the toughening of PLLA has become one of the most important issues in the field of biopolymer engineering.^{1,6} Blending with a ductile polymer is known as an effective way to improve the toughness of a base brittle polymer. In addition, blending may be used to reduce the cost of an expensive engineering thermoplastic polymer and to improve the processability of a high-temperature or heat-sensitive thermoplastic. The blending of PLLA with other biodegradable polyesters has been reported in previous research.^{1,4,8–11} It has been found that blending PCL with PLLA increases ductility and, therefore, improves the fracture toughness of PLLA.¹

In this study, a comparison of PLLA/PCL and PLLA/PBSL blends was made with blending ratios of 100/0, 90/10, 80/20, 70/30, and 0/100 (based on the weight percentage). Various characterization methods such as tensile and flexural testing, dynamic mechanical analysis (DMA), differential scanning calorimetry (DSC) analysis, thermogravimetric analysis (TGA), melt flow index (MFI) analysis, Fourier transform infrared (FTIR), and morphological studies were carried out to compare the characteristics of these two

Correspondence to: M. Mariatti (mariatti@eng.usm.my).

Contract grant sponsor: Asean University Network/Southeast Asia Engineering Education Development Network and Japan International Cooperation Agency; contract grant number: 6050131.

blends. The main aim of this study was to improve the brittleness of PLLA with the blending method with two types of ductile biodegradable polymers, such as PCL and PBSL.

EXPERIMENTAL

Materials

Medical-grade PLLA pellets (Lacty 5000; weight-average molecular weight = 1.45×10^5) were supplied by Shimadzu Co., Ltd. PLLA is a thermal plastic material derived from lactic acid with a glass-transition temperature (T_g) around 57°C and a melting temperature (T_m) around 180°C . PCL pellets with a grade of Celgreen PH7 (weight-average molecular weight = 1.25×10^5) were supplied by Daicel Chemistry Industry, Ltd. The T_g and T_m values of PCL were -60 and 60°C , respectively. PBSL pellets (GS Pla AZ type; ca. 3% lactate unit; weight-average molecular weight = 1.47×10^5) were supplied by Mitsubishi Chemical Corp. The T_g and T_m values of PBSL were -33 and 113.6°C , respectively. Figure 1 shows the chemical structures of PLLA, PCL, and PBSL.

Blend preparation

The virgin PLLA and PLLA polymer blends were prepared by melt mixing in a two-roll mill heater machine at 190°C for 10 min. However, because of differences in the thermal properties, the virgin PCL and PBSL were melted at 70 and 120°C , respectively. The PLLA/PCL and PLLA/PBSL blend ratios used in this study included 0/100, 90/10, 80/20, 70/30, and 100/0 (based on the weight percentage). PLLA was charged into the two-roll mill and was allowed to melt for 4 min. Then, PCL or PBSL was added to the molten PLLA, and the mixing was continued for another 6 min. The samples were then compression-molded at the same temperature as the processing

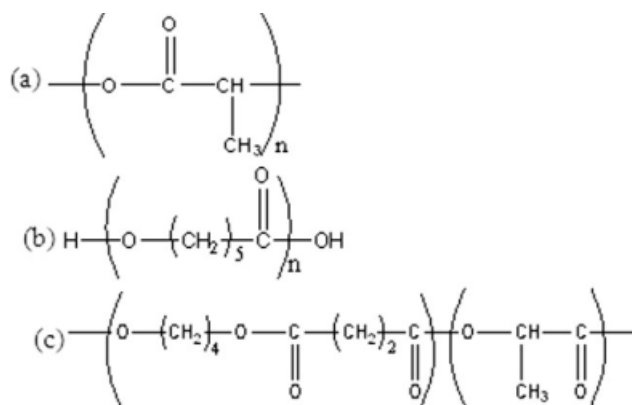


Figure 1 Chemical structures of (a) PLLA, (b) PCL, and (c) PBSL.

temperature in the two-roll mill heater machine for 7 min, and this was followed by cooling.

Measurements

FTIR measurements were carried out with a PerkinElmer (Waltham, MA) Spectrum One spectrometer with a resolution of 2 cm^{-1} for four scans over a wave-number range of $4000\text{--}400\text{ cm}^{-1}$. The samples were obtained via the casting of films of polymer resolution on a KRS-5 disc. The solvent (chloroform) was evaporated at room temperature for at least 5 min before the IR spectra were recorded.

MFI measurements were obtained with a Dynisco (Franklin, MA) model D4004 HV polymer tester according to ASTM D 1238-04c (procedure A, $190^\circ\text{C}/2.16\text{ kg}$). The molten polymer was allowed to flow through an orifice for 1 min, and the extruded plastic was then weighed. MFI was the output rate ($\text{g}/10\text{ min}$) from a standard die (2.1 mm in diameter and 8.0 mm long).

Mechanical property testing, such as tensile and three-point flexural testing, was performed with an Instron (Norwood, MA) 3366 universal mechanical testing machine according to ASTM D 638 type I and ASTM D 790, respectively. Tensile and flexural testing was performed at a crosshead speed of $50\text{ mm}/\text{min}$. For flexural testing, the span length was fixed at 16 times the thickness of the span configuration. For all testing measurements, at least five specimens were tested to obtain the average and standard deviation.

The dynamic mechanical properties of the samples were measured with a Mettler–Toledo (Columbus, OH) model DMA 861 in a dual-cantilever mode at a frequency of 1 Hz. The temperature was increased at $5^\circ\text{C}/\text{min}$ over the range of -100 to 150°C . The dimensions of the samples were approximately $50\text{ mm} \times 12\text{ mm} \times 3\text{ mm}$. TGA was conducted with a PerkinElmer Pyris 6 TGA analyzer. The temperature range of $30\text{--}650^\circ\text{C}$ at a heating rate of $10^\circ\text{C}/\text{min}$ under a nitrogen atmosphere was used. DSC was used to determine the T_m and T_g values of the virgin and blend samples with a PerkinElmer DSC-7 system. Approximately 8–10 mg of the samples was weighed and put into an aluminum pan with a cover. The samples were then scanned from -70 to 210°C at a scan rate of $10^\circ\text{C}/\text{min}$ and held for 1 min at 210°C , and this was followed by the cooling process from 210 to -70°C at $20^\circ\text{C}/\text{min}$. The second cycle was carried out at the same heating rate to determine the thermal properties of the samples. The intrinsic degree of crystallinity [$X_{c,\text{PLLA}}$ (%)] was determined with Eq. (1):

$$X_{c,\text{PLLA}} (\%) = \frac{(\Delta H_c - \Delta H_m) \times 100}{93 \times X_{\text{PLLA}}} \quad (1)$$

where ΔH_c and ΔH_m are the enthalpies of crystallization and melting of PLLA, respectively; the constant of 93 J/g is the fusion enthalpy of PLLA;^{1,12} and X_{PLLA} is the weight fraction of PLLA.

Field emission scanning electron microscopy (FESEM) of the cryofractured surfaces was performed with a Leo Supra 35VP (Oberkochen, Germany) to characterize the phase morphology of the PLLA blends. The fracture surfaces were obtained by immersion of the materials in liquid nitrogen (N_2) for about 30 min. These fracture surfaces were then coated by sputtering with gold. FESEM of the fracture surfaces of the tensile test specimens was also performed to characterize the failure mechanisms under tensile loading conditions.

RESULTS AND DISCUSSION

FTIR spectroscopy analysis

Figure 2 shows the FTIR spectra of PLLA, PCL, PBSL, and PLLA/PCL (80/20 wt %) and PLLA/PBSL (80/20 wt %) binary blends. The FTIR scans clearly indicate that all of the systems had similar chemical bonding because of the presence of identical functional groups. The characteristic peak of the hydroxyl group ($-\text{OH}$) appears in the region of

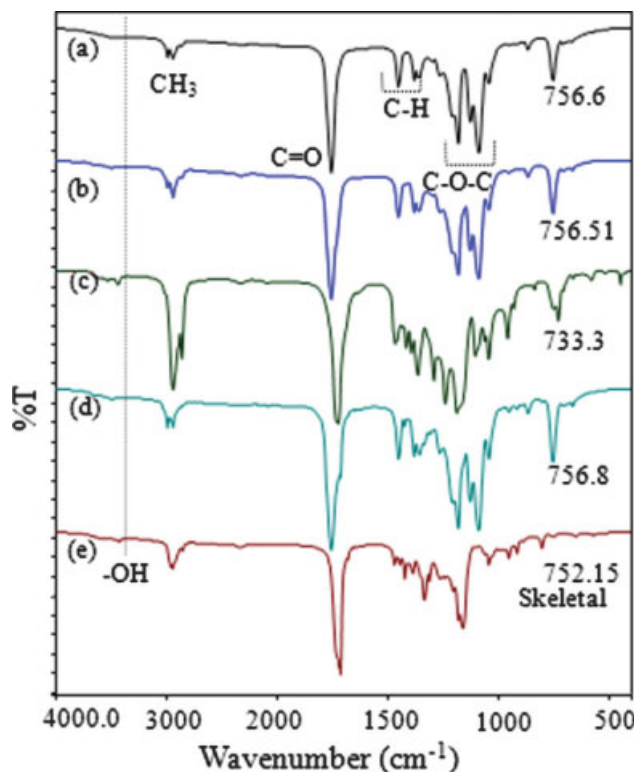


Figure 2 FTIR spectra of virgin polymers and polymer blends: (a) PLLA, (b) PLLA/PCL (80/20 wt %), (c) PCL, (d) PLLA/PBSL (80/20 wt %), and (e) PBSL. [Color figure can be viewed in the online issue, which is available at www.interscience.wiley.com.]

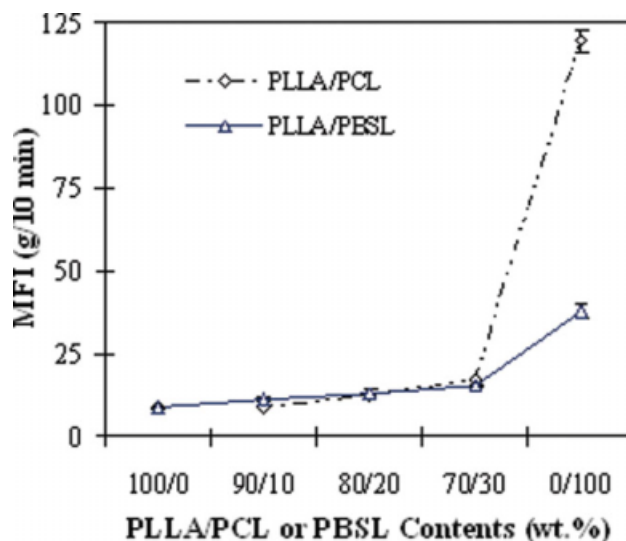


Figure 3 MFI values versus the PCL or PBSL content of PLLA/PCL and PLLA/PBSL blends. [Color figure can be viewed in the online issue, which is available at www.interscience.wiley.com.]

3440–3500 cm^{-1} in most of the spectra. As for the end group, their intensities consistently appeared quite weak because of their low molar content in the respective polymeric chains. Two distinct peaks in the region of 2850–2980 cm^{-1} correspond to the asymmetrical and symmetrical stretching modes of the CH_3 groups. Of note is the strong intensity for this peak in PCL, which consistently represents a higher molar content of the methyl group in comparison with the polymer blends. In all spectra, the $\text{C}=\text{O}$ group occurs in the region of 1751–1758 cm^{-1} , whereas that of $\text{C}-\text{O}-\text{C}$ occurs in the region of 1050–1200 cm^{-1} . Peaks in the region of 1430–1480 cm^{-1} represent $\text{C}-\text{H}$ deformation, whereas those at 733–756 cm^{-1} represent the skeletal vibration of the methylene groups.

MFI

Figure 3 shows the MFI values of PLLA, PCL, PBSL, and their blends. The virgin PCL and PBSL had higher MFIs than PLLA and their blends under the measurement conditions of a 2.16-kg load at 190°C. Because of the low T_m values of PCL and PBSL (ca. 60 and 112°C, respectively), they readily melted at an operating temperature of 190°C, and this induced a very low viscous fluid. Hence, this resulted in higher MFI values at about 119 and 38 g/10 min, respectively. On the other hand, PLLA ($T_m = 174^\circ\text{C}$) exhibited a high viscosity and a low MFI of 8.6 g/10 min under the processing conditions. The MFI values for the blended components increased with an increase in the PCL or PBSL content, indicating the similar viscosities observed in the blend systems.

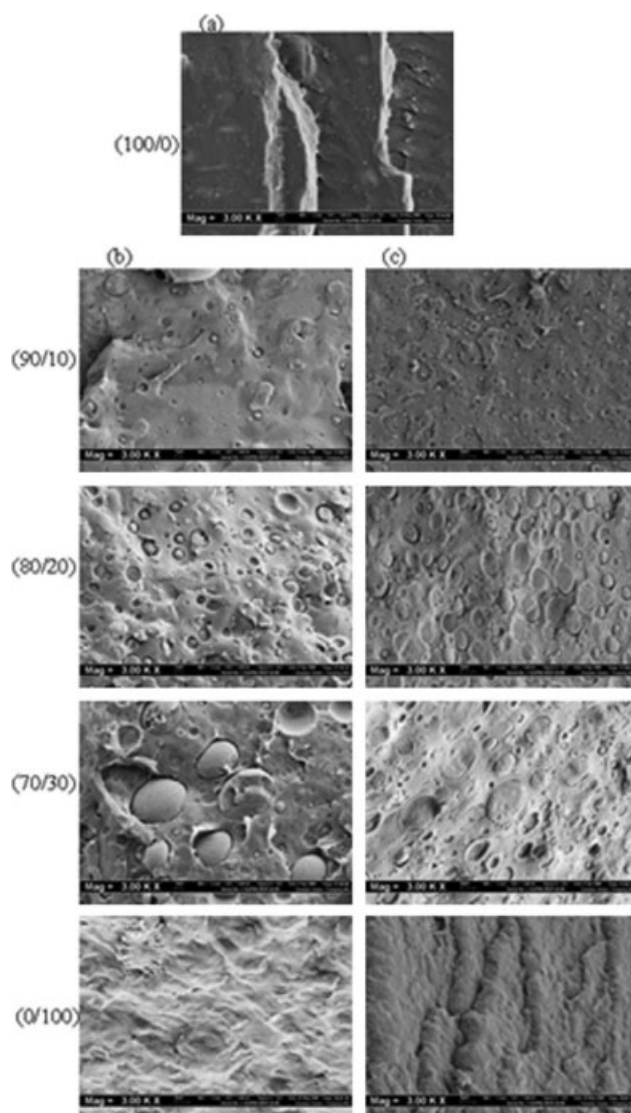


Figure 4 SEM micrographs of fractured surfaces under liquid N₂ of (a) PLLA and blends of (b) PLLA/PCL, and (c) PLLA/PBSL at various contents.

Their values, however, were almost the same, regardless of the PCL or PBSL components used.

Phase morphology

Figure 4 shows micrographs of the fractured surfaces of PLLA/PCL and PLLA/PBSL blends. The micrographs of the fractured surfaces show the morphology of the phase-separated system, with the dispersed PCL and PBSL phase having a spherical shape, particularly with 10–30 wt % PCL or PBSL. For the virgin PLLA, the final structure indicated brittleness [Fig. 4(a,b) at 100/0 wt %]. For the blends of all components, the size of the dispersed phase of PCL and PBSL increased with an increase in the contents of PCL and PBSL. A blend of immiscible polymers generally creates macrophase separation of the

two components because of the difference in the solubility parameters.¹ Stress concentration usually takes place in the vicinity of the dispersed phase separations because of differences in the elastic modulus between the dispersed phases and the surrounding matrix, and it initiates localized microdamage in this region. The phase separation subsequently affects the physical and mechanical properties of the blend.¹

Mechanical properties

Tensile properties

The increase in the ductility of the PLLA blend is clearly evident in the tensile stress–strain curves shown in Figure 5. The fracture of PLLA occurred immediately after the upper yield stress. The sample could not be drawn because the material showed only minimal plastic deformation. On the basis of the stress–strain curves, the virgin PBSL or PCL had a rather lower modulus than PLLA. By comparing the Young’s moduli of virgin PLLA, PBSL, and PCL, we could expect the addition of PCL or PBSL to reduce the Young’s modulus of the PLLA blends. Judging from the area under stress–strain curves, we found that PLLA showed less toughness than the PCL and PBSL polymers. The addition of 20 wt % PCL and PBSL to the PLLA matrix favorably improved the deformation behavior of the material. However, the upper yield stresses of the two blends were slightly similar. The drawability of the material markedly increased because of the plastifying effect of the amorphous mixed phase at the interphase of the PLLA/PCL and PLLA/PBSL blends and because of the reduced matrix crystallinity. The local deformation in the deformation region after the upper yield stress was characterized by a reduction in the

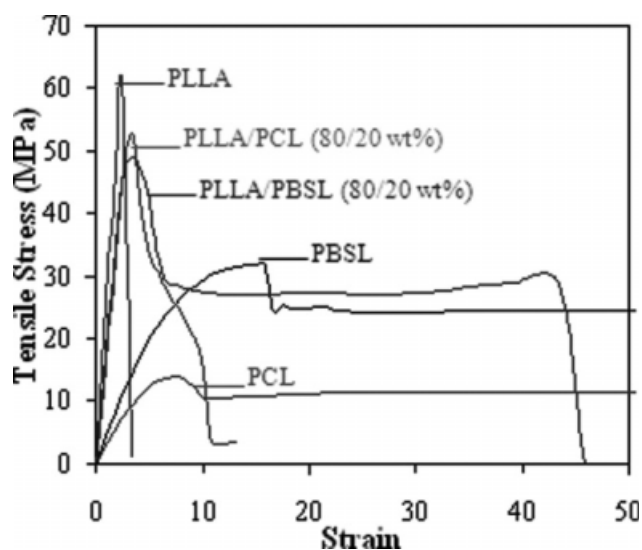


Figure 5 Tensile stress–strain curves (the strains at break of PCL and PBSL were 5.7 and 2.1 mm/mm, respectively).

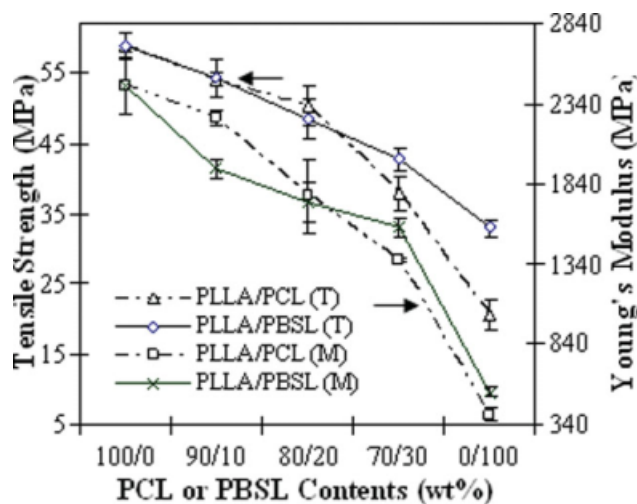


Figure 6 Tensile strength (T) and Young's modulus (M) versus the PCL or PBSL content of PLLA, PCL, PBSL, and PLLA/PCL and PLLA/PBSL blends. [Color figure can be viewed in the online issue, which is available at www.interscience.wiley.com.]

local cross section (neck). Before the fracture, small strain hardening could be seen, and the material broke at maximal deformation. This strain hardening was caused by the orientation of the PLLA chains parallel to the drawing axis.

Figure 6 shows the tensile strength and Young's modulus of the polymers and their blends. PLLA showed a higher tensile strength and Young's modulus than PCL, PBSL, and the blended components. The tensile strength and modulus of the blend formulations decreased with a decrease in the PLLA content. This indicated that PCL and PBSL did not enhance the tensile properties of PLLA. The blends approximately followed the rule of mixtures over

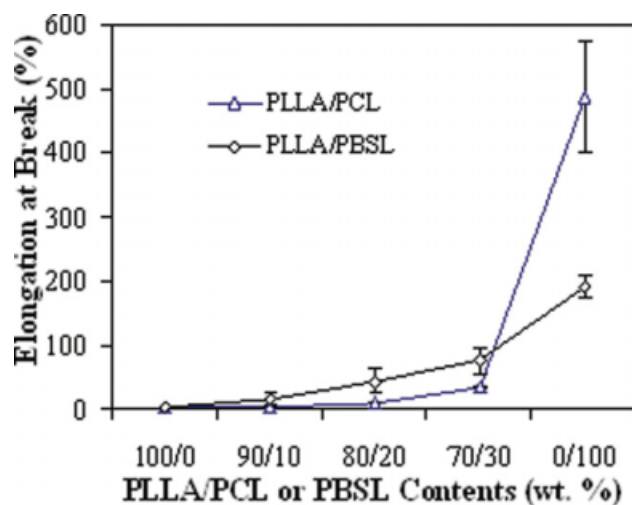


Figure 7 Elongation at break versus the PCL or PBSL content for PLLA/PCL and PLLA/PBSL blends. [Color figure can be viewed in the online issue, which is available at www.interscience.wiley.com.]

the whole composition range; that is, the properties of the blends were usually between those of their constituents. The phase separation leading to the formation of voids could be observed clearly in the PLLA/PCL blends, and this explained the obvious drop in the tensile strength of the PLLA/PCL blends with a higher PCL content in comparison with the PLLA/PBSL blends. The result agrees with previous work by Shibata et al.,⁹ who noted that the tensile strength and modulus of blends are between the properties of the pure polymers.

As expected, the elongation at break of the PLLA/PCL and PLLA/PBSL blends increased with an increase in the PCL and PBSL contents, as shown in Figure 7. The virgin PLLA was brittle, and this indicated an elongation at break of about 2%. The virgin PCL exhibited a higher elongation at break (ca.

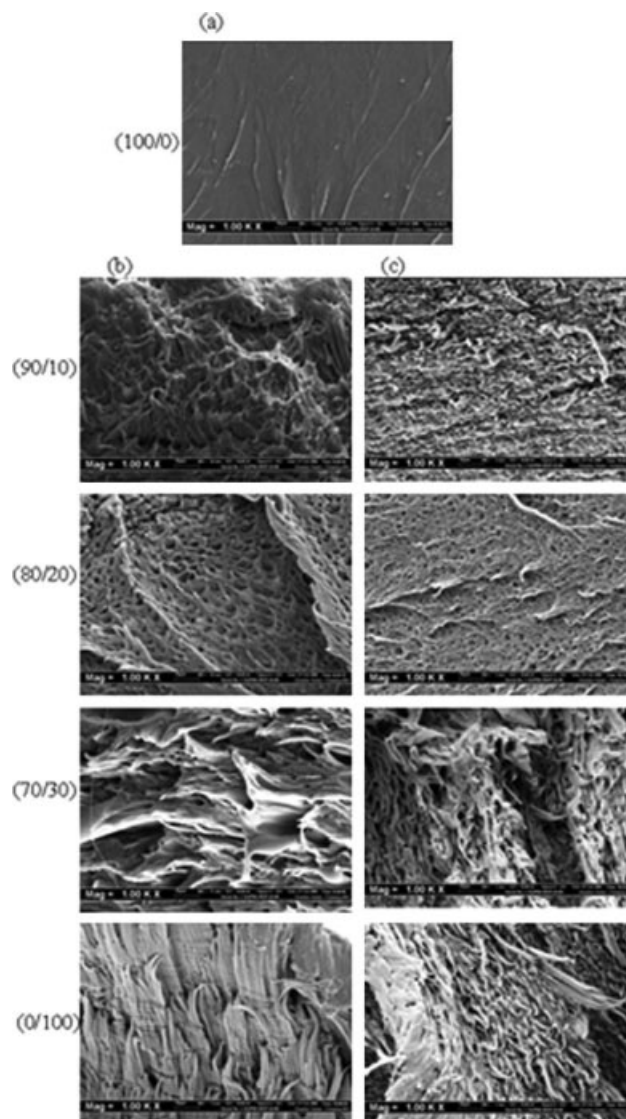


Figure 8 SEM micrographs of tensile-fractured surfaces of (a) PLLA and blends of (b) PLLA/PCL, and (c) PLLA/PBSL at various blend ratios.

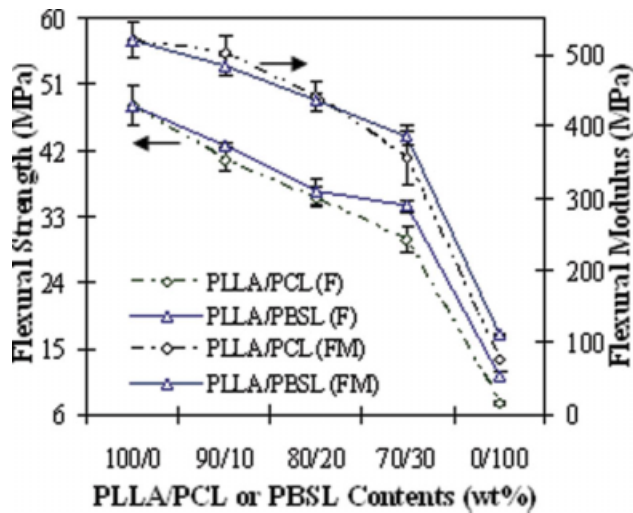


Figure 9 Flexural strength (F) and flexural modulus (FM) versus the PCL or PBSL content of PLLA/PCL and PLLA/PBSL blends. [Color figure can be viewed in the online issue, which is available at www.interscience.wiley.com.]

450%) in comparison with the virgin PBSL (ca. 200%) and the blend systems. According to a previous study,¹³ the flexibility of PCL and PBSL can be explained by the long aliphatic groups in the backbones of the PCL and PBSL molecules (cf. the PLLA, PBSL, and PCL structures in Fig. 1). This results in the low density of the rigid carboxyl bond in comparison with PLLA. As a result, the chains can easily slip during deformation, so despite higher crystallinity, PCL and PBSL are flexible and tough.

The elongation at break of the PLLA/PCL blends was lower than that of PLLA/PBSL, and this might be due to the obvious phase separation occurring in the PLLA/PCL blends in comparison with the PLLA/PBSL blends (as shown in Fig. 4). On the basis of the fracture morphology shown in Figure 7, it is apparent that PCL and PBSL showed plastic deformation behavior, as indicated by the formation of a fibril structure. The fibril formation supported the results of higher elongation at break of the PCL and PBSL

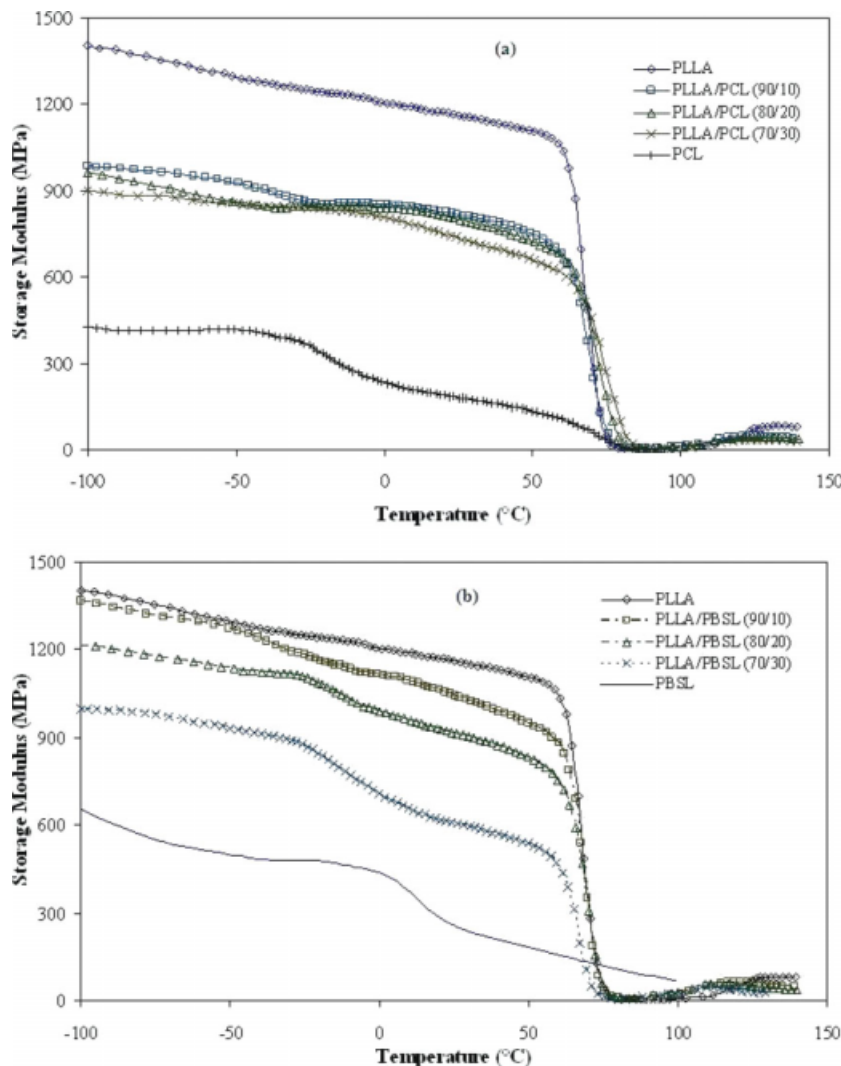


Figure 10 Plots of the storage modulus versus the temperature for (a) PLLA/PCL and (b) PLLA/PBSL blends. [Color figure can be viewed in the online issue, which is available at www.interscience.wiley.com.]

polymers. The fibril structures slightly disappeared with an increase in the amount of PLLA. The brittle morphology of PLLA is obviously shown in Figure 8 for a ratio of 100/0, indicating the brittle fracture behavior of the virgin PLLA. The plastic morphology shown by the SEM images is in accordance with the results of tensile testing. These indicate that the blending of PLLA with PCL and PBSL improved the elongation at break and toughness of PLLA.

Flexural properties

The flexural strength and modulus of the virgin polymers and their two binary blends were investigated and are shown in Figure 9. As expected, PLLA had the highest flexural strength and modulus in comparison with the PLLA/PCL and PLLA/PBSL blends.

The incorporation of PCL and PBSL into the PLLA blends decreased the flexural strength and modulus. These trends resembled those of the tensile properties. This reduction in the flexural properties could be again attributed to the poor interaction of PCL or PBSL in the PLLA blends (as shown in Fig. 5).

Thermal properties

DMA

Plots of the storage modulus of two blended systems (PLLA/PCL and PLLA/PBSL) as a function of temperature, obtained from DMA, are shown in Figure 10(a,b), respectively. The stepwise storage modulus decreased with an increase in the PCL or PBSL content for the blends [Fig. 10(a,b)]. For the virgin PLLA, the storage modulus fell abruptly at approximately

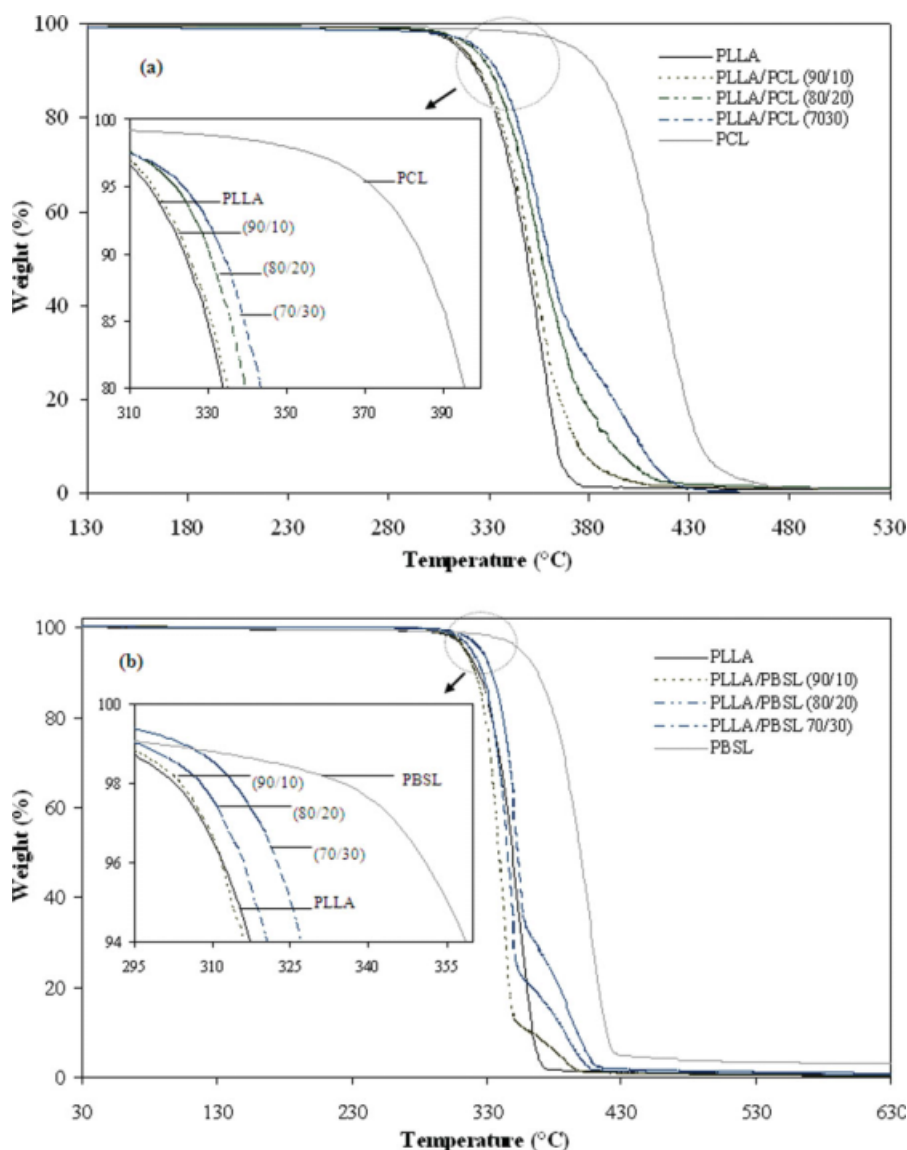


Figure 11 TGA data for PLLA blends prepared with various contents of (a) PCL and (b) PBSL. [Color figure can be viewed in the online issue, which is available at www.interscience.wiley.com.]

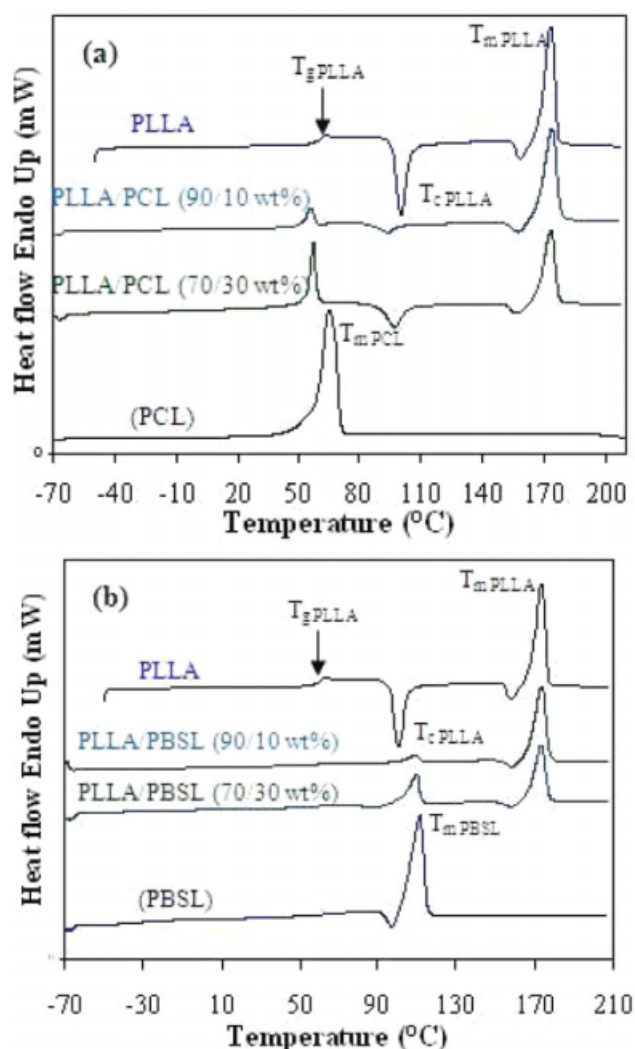


Figure 12 DSC curves of heating thermograms of (a) PLLA/PCL and (b) PLLA/PBSL blends. [Color figure can be viewed in the online issue, which is available at www.interscience.wiley.com.]

62°C, representing the onset of the glass transition, and then rose around 100°C because of crystallization. The results are in accordance with previous works.^{6,9} For 10, 20, and 30 wt % PCL or PBSL, the decreasing trend occurred at approximately 61, 59, and 57°C, respectively. However, for virgin PCL and PBSL, the transitions seemed to occur over a broader range of temperatures. At -100°C, PLLA showed a storage modulus of approximately 1401 MPa. The addition of 10, 20, and 30 wt % PCL and PBSL resulted in a decrease of these values to 984, 963, and 897 MPa (1365, 1217, and 997 MPa), respectively. PLLA/PCL showed a lower storage modulus than PLLA/PBSL (with a similar blend ratio) and exhibited small differences in the storage modulus with 90/10, 80/20, and 70/30 blend ratios. This might be due to the obvious phase separation occurring in the PLLA/PCL blend systems (as shown in Fig. 4), which reduced the stor-

age modulus of the blends. The addition of PCL and PBSL was expected to decrease the storage modulus of the PLLA blends because of the lower storage moduli of virgin PCL and PBSL (425 and 655 MPa, respectively).

TGA

Figure 11(a,b) shows the TGA data of the PLLA/PCL and PLLA/PBSL blends, respectively, with various blend ratios. In general, both types of polymer blends showed similar thermal stability ranges. The thermal onset degradation temperatures of PLLA, PCL, and PBSL showed a simple decomposition profile in a single step and were about 358, 418, and 411°C, respectively. Meanwhile, both PLLA/PCL and PLLA/PBSL blends were characterized by two degradation steps; the step range increased correspondingly with the PCL or PBSL content in the blends. Despite PLLA and PCL or PBSL having similar molecular structures, these degradation steps indicated the existence of two distinct and immiscible phases derived from the PLLA matrix and the PCL or PBSL dispersed phase. PCL and PBSL showed higher thermal stability than PLLA and the blends. The PLLA/PCL blends prepared with various contents of PCL revealed that the introduction of PCL to the PLLA matrix resulted in thermal stability ranging between those of the two components [Fig. 11(a)]. This increase in the thermal stability was observed with the increase in the PCL content. The same trend was observed in the PLLA/PBSL blends, as shown in Figure 11(b).

DSC

Figure 12 shows the DSC curves for the second heating thermograms of each polymer and the PLLA/PCL and PLLA/PBSL blends. The crystallization temperature (T_c) and the degree of crystallinity of various compositions of PCL or PBSL are summarized in Table I. In the virgin PLLA thermogram [Fig.

TABLE I
Degree of Crystallinity of Virgin PLLA and PLLA/PCL and PLLA/PBSL Blends by DSC

Material	$T_{c, PLLA}$ (°C)	$\Delta H_{c, PLLA}$ (J/g)	$\Delta H_{m, PLLA}$ (J/g)	$X_{c, PLLA}$ (%)
PLLA/PCL				
100/0	100.54	28.998	56.077	91.478
90/10	93.71	5.791	41.032	55.941
70/30	97.22	12.764	29.93	65.586
0/100	—	—	—	—
PLLA/PBSL				
90/10	—	—	8.352	—
70/30	89.18	2.399	28.018	46.723
0/100	—	—	—	—

12(a,b)], the heat jump corresponding to T_g of PLLA occurred at about 61°C, and this was followed by a cold crystallization exotherm at about 100°C and a melting peak at about 174°C. DSC of the virgin PCL and PBSL revealed that their T_m values were about 64 and 111°C, respectively. However, the phase transition or T_g of PCL and PBSL could not be seen clearly from the curves. However, the T_g values of PCL and PBSL were -64.7 and 32.9°C, respectively. The peak at about 64–66°C observed for the PLLA/PCL blend could be attributed to the overlapping of the glass transition of PLLA and the melting peak of PCL. Both blend systems showed melting peaks of PLLA at about 174°C. In addition, the blends and virgin PLLA presented two exothermic peaks, the former appearing at 100°C, which could be attributed to a typical cold crystallization of PLLA, and the second appearing just before the melting point of PLLA. This peculiar exothermic event before the melting point has been observed in PLLA under certain crystallization conditions. According to a recent study,¹⁴ this phenomenon can be explained by the possibility of recrystallization of the lower perfection crystals of polylactide into the α crystal of higher perfection ones. In the PLLA/PBSL blends, overlapping of T_c of PLLA and T_m of PBSL occurred at about 100°C.

The level of crystallinity (X_c) of virgin PLLA and PLLA blends with PCL and PBSL was calculated with Eq. (1) and is reported in Table I. The virgin PLLA showed a higher X_c value than the blends. X_c of PLLA decreased with the addition of PCL. The presence of PCL interfered with the crystallinity of PLLA, hence reducing X_c of the blends. Most of the X_c data for PLLA/PBSL could not be measured because of the overlapping phenomena of T_c (PLLA) and T_m (PBSL) occurring in the blend systems; hence, the observed data were not really representative of the crystallinity of PLLA.

CONCLUSIONS

PLLA and PLLA blends with various compositions of PCL and PBSL were prepared via a two-roll mill

technique. The addition of the PCL and PBSL polymers not only increased the elongation at break and the MFI values but also enhanced the toughness and thermal stability of the PLLA polymer. The SEM micrograph showed the microphase separation of the PLLA/PCL and PLLA/PBSL blends, which indicated the immiscibility of the polymer blends. As expected, the storage modulus of the PLLA blends decreased with the addition of PCL and PBSL. The crystallization process of PLLA was hindered by the addition of PCL, and this reduced the X_c values of the blends in comparison with that of PLLA. In general, the PLLA/PBSL blends showed higher mechanical and thermal properties than the PLLA/PCL blends. PLLA/PBSL with ratios of 90/10, 80/20, and 70/30 could be investigated further for applications in biopolymer engineering applications because of their higher mechanical and thermal properties in comparison with other polymer blends.

The authors greatly acknowledge the support of Universiti Sains Malaysia and Kyushu University.

References

1. Todo, M.; Park, S.-D.; Takayama T.; Arakawa, K. *Eng Fract Mech* 2007, 74, 1872.
2. Park, S. D.; Todo, M.; Arakawa, K.; Takenoshita, Y. *Key Eng Mater* 2005, 297, 2453.
3. Kobayashi, S.; Sugimoto, S. *J Solid Mech Mater Eng* 2008, 2, 15.
4. Shibata, M.; Inoue, Y.; Miyoshi, M. *Polymer* 2007, 48, 2768.
5. Ray, S. S.; Bousmina, M. *Prog Mater Sci* 2005, 50, 962.
6. Nakano, S.; El Salmawy, A.; Nakamura, T.; Kimura, Y. *Sen'i Gakkaishi* 2002, 58, 209.
7. He, A.; Han, C. C.; Yang, G. *Polymer* 2004, 45, 8231.
8. Wu, C.-S.; Liao, H.-T. *Polymer* 2005, 46, 10017.
9. Shibata, M.; Inoue, Y.; Miyoshi, M. *Polymer* 2006, 47, 3557.
10. Van de Velde, K.; Kiekens, P. *Polym Test* 2002, 21, 433.
11. Nakano, S.; El Salmawy, A.; Nakamura, T.; Kimara, Y. *Sen'i Gakkaishi* 2002, 50, 209.
12. Tsuji, H.; Mizuno, A.; Ikada, Y. *J Appl Polym Sci* 1998, 70, 2259.
13. Chen, B.; Sun, K. *Polym Test* 2005, 24, 978.
14. Zhang, J.; Duan, Y.; Sato, H.; Tsuji, H.; Noda, I.; Yan, S.; Ozaki, Y. *Macromolecules* 2005, 38, 8012.